ANTIOXIDANTS & REDOX SIGNALING
Volume 13, Number 6, 2010

DOI: 10.1089/ars.2009.2880

ORIGINAL RESEARCH COMMUNICATION

Redox State of the Endoplasmic Reticulum Is Controlled by *Ero*1L-alpha and Intraluminal Calcium

Balázs Enyedi, Péter Várnai, and Miklós Geiszt

Abstract

Formation of intra- and intermolecular disulfide bonds is an essential step in the synthesis of secretory proteins. In eukaryotic cells, this process occurs in the endoplasmic reticulum (ER) and requires an oxidative environment with the action of several chaperones and folding catalysts. During protein folding, *Ero*1p oxidizes protein disulfide isomerase (PDI), which then directly catalyzes the formation of disulfide bonds in folding proteins. Recent cell-free studies suggest that the terminal electron acceptor in the pathway is molecular oxygen, with the resulting formation of hydrogen peroxide (H_2O_2). We report for the first time the measurement of ER H_2O_2 level in live cells. By targeting a fluorescent protein–based H_2O_2 sensor to various intracellular compartments, we show that the ER has the highest level of H_2O_2, and this high concentration is well confined to the lumen of the organelle. Manipulation of the *Ero*1-Lα level—either by overexpression or by siRNA-mediated inhibition—caused parallel changes in luminal H_2O_2, proving that the activity of *Ero*1-Lα results in H_2O_2 formation in the ER. We also found that calcium mobilization from intracellular stores induces a decrease in ER H_2O_2 level, suggesting a complex interplay between redox and calcium signaling in the mammalian ER. *Antioxid. Redox Signal.* 13, 721–729.

Introduction

Disulfide bond formation is an essential step in the synthesis of secretory proteins. The catalytic events of protein folding take place in the ER (13). Our best understanding of oxidative protein folding originates from studies on yeast in which the thiol oxidase *Ero*1p was identified as an essential protein in the process (9, 21, 23). The FAD-bound *Ero*1p oxidizes protein disulfide isomerase (PDI), which then directly catalyzes the formation of disulfide bonds in folding proteins. Cell-free studies suggest that the final electron acceptor in the pathway is molecular oxygen, which is finally reduced to hydrogen peroxide (H_2O_2) (12, 27).

The molecular details of protein folding in the mammalian ER are less clear, but mammalian homologues of *Ero*1p do exist and presumably play a role in protein folding similar to that observed in yeast (2). *Ero*1-Lα is present in several tissues, whereas *Ero*1-Lβ expression is characteristic for cells with high secretory capacity (19). Based on the mechanism of oxidative protein folding, it is assumed that the process imposes serious oxidative stress on cells that can be especially high in secretory cells, such as insulin-producing β cells or antibody-secreting plasma cells (3). Tu *et al.* (26) suggested that Ero1p activity could be responsible for $\geq$25% of total ROS production during protein synthesis. Despite the obvious significance of ER-associated ROS production, surprisingly little is known about this process. The scant amount of information on this issue is partially explained by the lack of adequate methods for the accurate, subcellular assessment of ROS production.

Recently Belousov *et al.* (1) introduced a novel fluorescent tool for measuring H_2O_2 in live cells. The probe HyPer was described to be specific for H_2O_2, because the sensor is based on the H_2O_2-sensing ability of the bacterial transcription factor OxyR (7). In this work, we targeted HyPer to different intracellular organelles and measured H_2O_2 concentration at these sites. Here we show that, among the organelles examined, the lumen of the ER contains the highest level of H_2O_2. The high level of H_2O_2 is well confined to the lumen of the ER and does not radiate beyond the luminal surface. We also showed that manipulation of *Ero*1-Lα level—either by overexpression or by siRNA-mediated inhibition—caused parallel changes in luminal hydrogen peroxide concentration. Furthermore, we demonstrate that depletion of intracellular calcium stores induces a decrease in the ER hydrogen peroxide level.

Materials and Methods

Materials

Histamine, thapsigargin, *N*-ethylmaleimide, 4,6-diamidino-2-phenylindole (DAPI), and DTT were purchased from Sigma

Department of Physiology, Semmelweis University, Faculty of Medicine, Budapest, Hungary.

(St. Louis, MO). Fura-PE3 acetoxymethyl ester was obtained from TEFLABS (Austin, TX). Anti-rabbit horseradish peroxidase and anti-mouse horseradish peroxidase were from Amersham Biosciences (Piscataway, NJ); polyclonal anti-*Ero*1-Lα Antibody was from Cell Signaling (Danvers, MA); monoclonal anti-PDI antibody was from Abcam (Cambridge, MA); monoclonal anti beta actin antibody was from Sigma; Alexa 568 monoclonal anti-mouse antibody was from Molecular Probes (Invitrogen, Carlsbad, CA); and monoclonal anti-V5 antibody was purchased from AbD Serotec (Martinsried, Germany).

DNA constructs, gene silencing

Vectors encoding HyPer (cytosolic) and HyPer-M (mitochondrial) described by Belousov *et al.* (1) were purchased from Evrogen (Moscow, Russia). HyPer was targeted to the cytoplasmic surface of the ER (HyPer-ER$_{cyto}$), to the nucleus (HyPer-3NLS), and to the plasma membrane (HyPer-PM) by using the following target sequences fused to the C terminus of the protein through a short linker (ANSRV). HyPer-ER$_{cyto}$: localization signal of *Saccharomyces cerevisiae* ubiquitin conjugase 6 (MVYIGIAIFLFVGLFMK); HyPer-3NLS: SV40 T-antigen NLS in triplicate (DPKKKRKV)$_3$; and HyPer-PM: C-terminal CAAX domain of human K-Ras (KMSKDVKK KKKKSKTKCVIM). For targeting HyPer to the lumen of the ER (HyPer-ER$_{lum}$), the HyPer cDNA was subcloned into the pCMV/myc/ER/GFP (Invitrogen) vector in place of the GFP fluorophore by using the *Pst*I and *Not*I restriction sites. This construct uses the N-terminal ER-target sequence of the murine Vh chain (MGWSCIILFLVATATGAHS) and a C-terminal KDEL retention signal for efficient ER targeting.

To create a vector encoding mCherry-ER, the GFP fluorophore of pCMV/myc/ER/GFP was replaced with mCherry by using the *Nhe*I *Not*I restriction sites. To create a vector encoding a mitochondrially targeted mRFP (mito-mRFP), the GFP fluorophore of pEF/myc/mito/GFP (Invitrogen) was replaced with mRFP by using *Pst*I and *Not*I restriction sites. This construct uses the N-terminal target sequence of the human cytochrome *c* oxidase VIII. subunit for efficient targeting. For targeting mRFP to the plasma membrane (PM2-mRFP), the N-terminal palmitoylation/myristoylation signal of the Lyn protein (MGCIKSKGKDSAGA) was used (15). A PCR fragment corresponding to the coding region of human *Ero*1-Lα mRNA was generated by using cDNA from human pulmonary fibroblast cells (Promocell, Heidelberg, Germany) as a template and the following oligonucleotides as primers: 5′-AAG CTG CCG GAG CTG CAA TGG-3′ and 5′-TTA ATG AAT ATT CTG TAA CAA GTT CCT GAA GT-3′. The PCR product was subcloned into the pcDNA3.1 V5-His-TOPO TA-cloning vector (Invitrogen). To create Ero1-Lα-mCherry, the construct was subcloned into a pmCherry-N1 vector by using *Xho*I and *Kpn*I restriction sites.

Synthetic *Ero*1-Lα RNAi duplexes (Stealth siRNA; Invitrogen) were obtained from Invitrogen for transient knockdown of *Ero*1-Lα. The sequences are as follows: *Ero*1-Lα-Si1: 5′-GGG ACA CAA CAU UAC AGA AUU UCA A-3′; *Ero*1-Lα-Si2: 5′-GGG CUU UAU CCA AAG UGU UAC CAU U-3′. A medium GC content control Stealth siRNA was used as negative control (Si-C). The same *Ero*1-Lα-Si1 and Si2 sequences were expressed as short hairpin RNAs by using the psiSTRIKE-hMGFP (Promega, Madison, WI) vector, following the manufacturer's instructions. Control siSTRIKE vectors were created by swapping three nucleotides in the specific siRNA sequences leading to the following sequences: Control *Ero*1-Lα-Si1, GGG ACg CAA CAa UAC AuA AUU UCA A; control *Ero*1-Lα-Si2,GGG CUg UAU uCA AAG UcU UAC CAU U. psiSTRIKE vectors were further modified by replacing the hMGFP fluorophore to mCherry by using *Nhe*I and *Bst*BI restriction sites.

A modified murine J chain (JcM) was created, as described by Mezghrani *et al.* (17). In brief, JcM was PCR amplified from cDNA prepared from murine spleen cells by using the primers 5′-ATG AAG ACC CAC CTG CTT CTC TGG-3′ and 5′-CGA TTC TTG CTA CCT TGA CTG CTC GAG C-3′. The PCR product was subcloned into the pcDNA3.1 V5-His-TOPO TA-cloning vector. With this protocol an extra cysteine was inserted between the J-chain coding region and the V5 tag. To enhance the expression of the protein, the construct was subcloned into the pcDNA 3.1(+) vector (Invitrogen) containing a GCCACC Kozak-sequence by using the *Kpn*I and *Eco*RI restriction sites. To increase the retention of the protein in the ER, a C-terminal KDEL sequence was added to the construct.

Single-amino-acid change mutants of HyPer (C199S corresponding to C121S in OxyR) and *Ero*1 (C394S) were created by using the Stratagene (La Jolla, CA) QuikChange site-directed mutagenesis kit, following the manufacturer's instructions. To identify mutant clones, silent mutations were also introduced in the QuikChange primers that were automatically designed by using the sequence-handling program "SeqHandler" (8).

All cloned, subcloned and mutated constructs were verified by sequencing.

Cell culture and transfection of cells

HeLa (CCL-2) cells were obtained from American Type Culture Collection (Manassas, VA) and maintained in Dulbecco's modified Eagle's medium (Lonza, Basel, Switzerland) supplemented with 10% fetal calf serum, 50 units/ml penicillin, and 50 μg/ml streptomycin in a 5% humidified CO_2 incubator at 37°C.

Cells were plated on six-well tissue-culture plates 1 day before transfections at a density of 2×10^5 cells/35-mm well for Western-blot and JcM-oxidation assays. For imaging experiments, cells were grown on 25-mm-diameter circular glass coverslips at a density of 1.5×10^5 cells/35-mm wells. Cells were transfected for 24 to 48 h with the indicated constructs (1 μg of total DNA/well) by using FuGene HD (Roche, Basel, Switzerland), according to the manufacturer's instructions. For RNAi experiments, Stealth siRNA duplexes (final concentration of 100 n*M*) were transfected for 48 h with Lipofectamine RNAiMAX reagent (Invitrogen), following the manufacturer's instructions.

Immunofluorescence, confocal analysis, and fluorescence measurements

Cellular nuclei were stained with DAPI and a standard immunofluorescent labeling protocol was used to stain PDI with Alexa568. Confocal images were collected on a Zeiss LSM510 confocal laser scanning microscope, equipped with a 63×1.4 oil immersion objective (Plan-Apochromat; Zeiss, Thornwood, NY) on a thermostated (37°C) stage. HyPer and

DAPI were excited with 488-nm argon and 405-nm violet diode lasers, respectively. Alexa568 and mRFP were excited with a 543-nm helium/neon laser. Emissions were collected by using a 500- to 530-nm bandpass filter for HyPer, 420- to 480- nm bandpass filter for DAPI, and a 560-nm longpass filter for Alexa568 and mRFP. Postacquisition picture analysis was performed by using the Photoshop (Adobe) software to expand to the full dynamic range, but only linear changes were allowed.

Fluorescence-intensity measurements were performed on an inverted microscope (Axio Observer, Zeiss) equipped with a 40×1.4 oil-immersion objective (Fluar, Zeiss) and a Cascade II camera (Photometrics, Tucson, AZ). Excitation wavelengths were set by a random-access monochromator connected to a xenon arc lamp (DeltaRAM, Photon Technology International, Birmingham, NJ). For ratiometric measurements of HyPer, excitation wavelengths of 490 and 420 nm were selected, combined with a 505-nm dichroic filter and a 525/36-nm emission filter set. Before the experiment, coverslips were placed into a chamber that was mounted on a heated stage, with the medium temperature kept at 37°C. Cells were incubated in 1 ml of a HEPES-buffered solution containing 145 m*M* NaCl, 5 m*M* KCl, 1 m*M* $MgCl_2$, 0.8 m*M* $CaCl_2$, 10 m*M* HEPES, 5 m*M* glucose, pH 7.4, and stimuli were added in 0.1 ml of prewarmed buffer after removing 0.1 ml of medium from the cells. The MetaFluor (Molecular Devices, Downingtown, PA) software was used for data acquisition. Images were acquired every 10 s for a period of 3 or 30 min. The 490/420-nm fluorescence excitation ratio of HyPer was calculated after background fluorescence subtraction.

The titration curve of HyPer was achieved by sequential addition of increasing concentrations of H_2O_2 to HeLa cells expressing HyPer-C. Mean fluorescence intensities over individual cells were calculated from 3-min recordings. For time-resolved measurements of fluorescence, background-subtracted recordings were averaged and plotted against time.

For parallel cytosolic calcium $[Ca^{2+}]_c$ and HyPer measurements, cells were loaded with Fura-PE3 (3 μM, 30 min, room temperature). Imaging was performed on the same filter setup as described before for HyPer, with additional excitations at 340 and 380 nm. Crosstalk between fluorophores was minimalized by measuring the Fura-PE3 ratio above the nuclei of the cells. Remaining crosstalk was calculated and subtracted, along with the background fluorescence. Images were acquired every 3 s for a period of 30 min.

Western blot experiments and JcM oxidation assay

Standard SDS-PAGE, Western-blot experiments were performed by using a 1:1,000 dilution of primary anti-Ero1-Lα, anti-actin, and anti-V5 antibodies, as described elsewhere (24). The JcM Oxidation Assay was performed as a modification of that described previously (17). In brief, JcM-V5 transfected HeLa cells were treated with 10 m*M* dithiothreitol (DTT) in DMEM and kept at 37°C for 20 min to achieve disulfide bond reduction. After two washing steps to eliminate DTT, oxidation was obtained by incubating cells at 37°C in DMEM. After 0, 1, 2, 4, and 8 min, oxidation was stopped by washing the cells with ice-cold PBS containing 10 m*M* *N*-ethyl maleimide (NEM). Cells were then lysed in Triton X-100 lysis buffer (1% Triton X-100, 50 m*M* Tris, 150 m*M* NaCl, 10 m*M* NEM, protease inhibitors) and processed in a standard non-reducing SDS-PAGE, Western-blot procedure.

For quantification of Western blots, the densitometry function of ImageJ 1.41 was used.

Statistics

Means ± SEM are shown. For estimating the significance of differences the Mann–Whitney rank sum test was used. Data were analyzed with Microsoft Excel and Sigmaplot 10.0 programs.

Results

Several cellular sources and biologic effects of H_2O_2 have been identified over the years, but defining the precise role of H_2O_2 in living organisms has been difficult due to the lack of specific techniques for H_2O_2 measurement. We decided to use a recently described protein-based H_2O_2 sensor, HyPer, to measure H_2O_2 at different subcellular sites of HeLa cells. The specificity of HyPer for H_2O_2 is based on its parent protein, OxyR, a prokaryotic H_2O_2-sensitive transcription factor (6). HyPer is a ratiometric probe: when it becomes oxidized by H_2O_2, the excitation peak at 420 nm decreases proportionate to the increase in the excitation peak at around 500 nm (1). The advantage of a ratiometric probe is that the fluorescent signal is independent of the amount of the expressed protein. We added different targeting sequences to HyPer and studied the intracellular localization of the recombinant proteins with confocal microscopy (Fig. 1). In the absence of a specific targeting tag, HyPer localized to the cytoplasm of HeLa cells (Fig. 1A). For targeting HyPer to the matrix of mitochondria (Fig. 1B), we used the method described by Belousov *et al.* (1). Nuclear localization was achieved by fusing the SV40 T-antigen nuclear-localization signal to the protein (Fig. 1C), and we used the CAAX domain of human K-Ras to send HyPer to the cytosolic surface of the plasma membrane (Fig. 1D).

We used two different strategies to target HyPer to the ER. For targeting to the lumen of the ER, we fused an N-terminal ER-target sequence of the murine Vh chain and a C-terminal KDEL retention signal to HyPer (Fig. 1E). Addition of the localization signal of *Saccharomyces cerevisiae* ubiquitin conjugase to HyPer resulted in localization to the cytoplasmic surface of ER (Fig. 1F). The specific localization of targeted HyPer proteins was confirmed by showing the colocalization of our probes with organelle-specific markers or fluorescent fusion proteins that were sent to the same compartment by using a different targeting strategy (Supplemental Fig. 1; *see* www.liebertonline.com/ars). Next we used single-cell fluorimetry for the ratiometric measurement of HyPer fluorescence, as described by Belousov *et al.* (1). Figure 1G shows that in the cytosol, nucleus, and on the cytoplasmic surface of the ER, the ratio was close to 1, indicating a low H_2O_2 concentration at these sites under resting conditions. In the matrix of the mitochondria, we observed a higher ratio (1.49 ± 0.03), which is well explained by the fact that H_2O_2 is formed as a byproduct of mitochondrial respiration. Among the organelles examined, we measured the highest fluorescence ratio in the lumen of the ER (3.10 ± 0.11). It is noteworthy that this high level of H_2O_2 is well confined to the lumen of ER and does not affect the H_2O_2 concentration measured at the cytoplasmic surface of the ER (Fig. 1G).

In our next experiments, we focused on the origin and regulation of the H_2O_2 level in the lumen of the ER. First, we

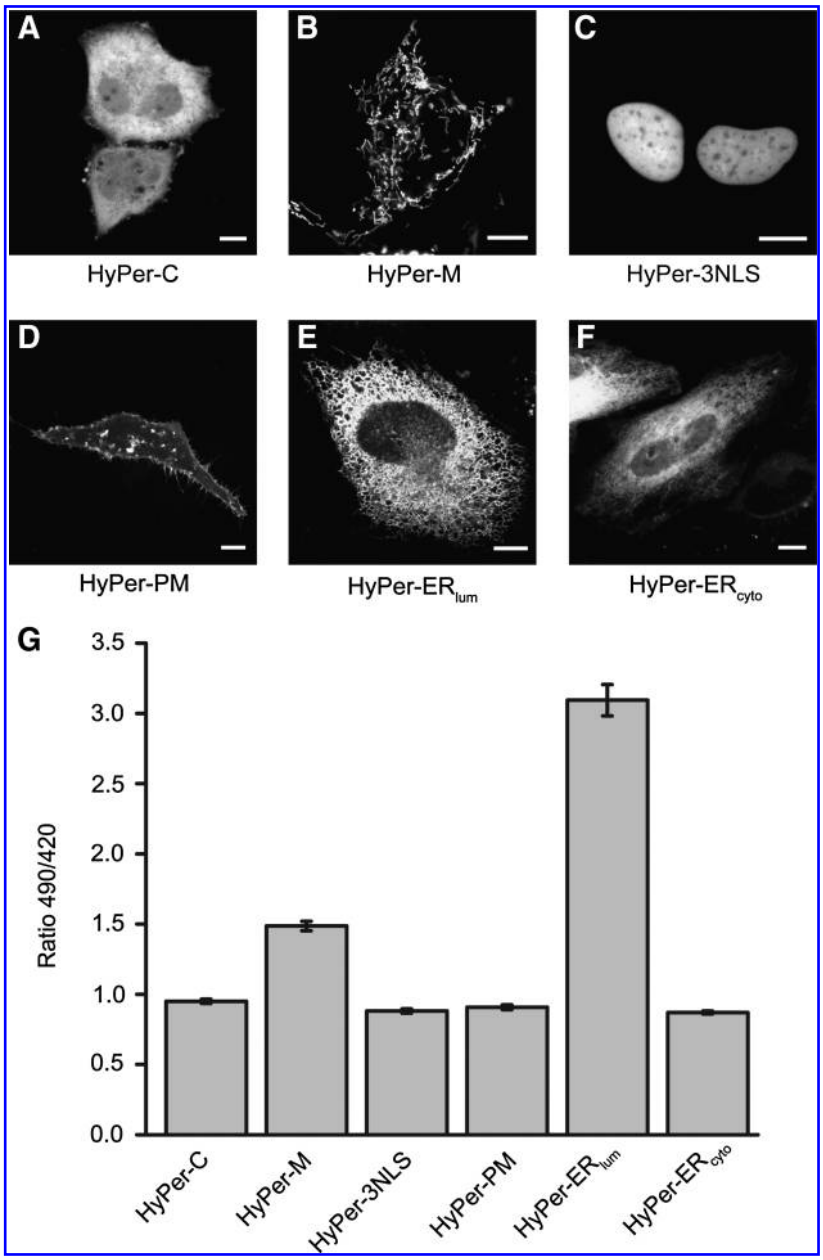

FIG. 1. Measurement of subcellular H_2O_2 levels by specifically targeted HyPer. Confocal images of HeLa cells expressing HyPer targeted to the cytosol (**A**) (HyPer-C), mitochondria (**B**) (HyPer-M), nucleus (**C**) (HyPer-3NLS), cytosolic surface of the plasma membrane (**D**) (HyPer-PM), lumen of the endoplasmic reticulum (**E**) (HyPer-ER$_{lum}$), and the cytosolic surface of the endoplasmic reticulum (**F**) (HyPer-ER$_{cyto}$). White bars represent 10 μm. (**G**) The 490/420-nm fluorescence excitation ratio of HyPer expressed in various cellular organelles of HeLa cells. Bars represent mean values ± SEM of 43–103 cells from four independent experiments.

determined that the fluorescence ratio measured in the ER corresponds to the fluorescence ratio of HyPer in the cytosol stimulated with 90 μM H_2O_2 (Fig. 2A), suggesting that the concentration of H_2O_2 in this organelle might reach levels this high. Next, we studied the effect of the reducing agent DTT on the fluorescent signal (Fig. 2B). The addition of 0.5 mM DTT to cells expressing HyPer-ER$_{lum}$ induced a rapid decrease in fluorescence, indicating that the fluorescent signal truly reflects the oxidative state of the ER. When we washed out DTT from the medium, the signal recovered quickly to the proximity of the original level (Fig. 2B). The small difference between the original and the recovered signal is probably due to the presence of some residual DTT in the ER. The addition of 100 μM H_2O_2 to the cells rapidly restored the signal above the original level, whereas it did not affect the localization of the probe (Supplemental Fig. 2; *see* www.liebertonline.com/ars). Addition of 0.5 mM DTT to cells expressing cytosolic HyPer had no effect on the fluorescent signal, indicating that, under resting conditions, cytosolic HyPer is in a reduced state. When these cells were treated with 100 μM H_2O_2, the fluorescence ratio increased to the level observed in cells expressing HyPer-ER$_{lum}$ (Fig. 2B).

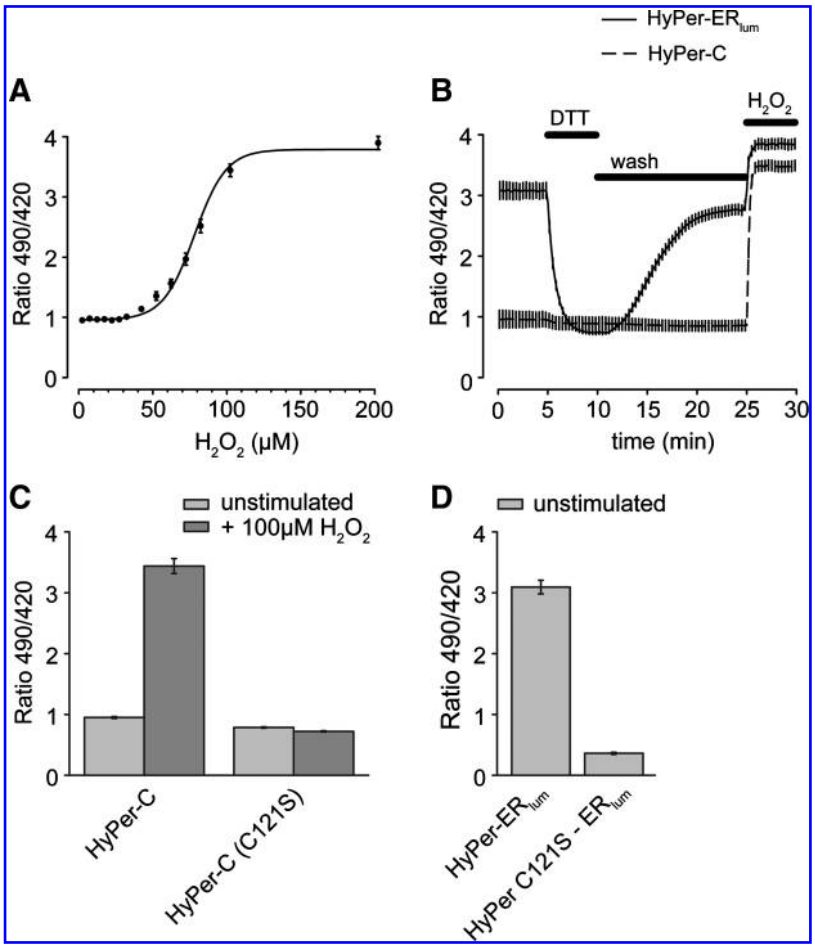

FIG. 2. Specific cysteine residues are oxidized in ER-targeted HyPer. (**A**) H_2O_2 titration curve of HyPer-C acquired in HeLa cells, as described in Materials and Methods ($n = 42$ cells from three independent experiments). (**B**) HeLa cells expressing HyPer-ER$_{lum}$ or HyPer-C were perfused for 5 min with 0.5 m*M* DTT; then DTT was washed out of the medium for the indicated time. Cells were treated with 100 μM H_2O_2 at the end of the experiment. Mean ± SEM are shown ($n = 26$ and 16 cells from three independent experiments on HyPer-ER$_{lum}$ and HyPer-C, respectively). (**C, D**) The 490/420-nm fluorescence ratios were recorded for 3 min on HeLa cells expressing HyPer-C ($n = 46$), HyPer-C(C121S) ($n = 91$), HyPer-ER$_{lum}$ ($n = 85$), or HyPer-ER(C121S)$_{lum}$ ($n = 60$) under basal conditions or after stimulation with 100 μM H_2O_2. Mean ± SEM from four independent experiments on the given number of cells (n) is shown.

Next we studied whether the high fluorescent signal in the ER is indeed a consequence of the oxidation of specific cysteine residues in a H_2O_2-sensing "pocket" of HyPer (6). To examine this, we first created a mutant version (C121S) of cytosolic HyPer. Figure 2C shows that the addition of H_2O_2 to cells expressing the wild-type protein induced a large increase in fluorescence, whereas the mutant version of the protein was insensitive to H_2O_2. When the C121S mutant version of HyPer was targeted to the ER, we measured a much lower fluorescence ratio compared to the signal observed with the wild-type protein (Fig. 2D). These experiments have proven that the high fluorescence ratio observed in the ER is indeed the consequence of the high H_2O_2 concentration in this organelle.

Next we studied the possible origin of the high H_2O_2 level in the ER. Cell-free studies using components of the yeast protein-folding machinery demonstrated that the action of *Ero*1 proteins results in formation of H_2O_2 (12, 27). Because this activity of *Ero*1 has never been demonstrated in live cells, we manipulated the *Ero*1-Lα level in HeLa cells and studied the consequent changes in HyPer fluorescence (Fig. 3). The expression level of the *Ero*1-Lα protein was determined with Western blot analysis (Fig. 3A). *Ero*1-Lα was then tagged with mCherry, to allow its visualization during coexpression with HyPer-ER$_{lum}$ (Supplemental Fig. 3; *see* www.liebertonline.com/ars). As shown in Fig. 3B, overexpression of *Ero*1-Lα increased HyPer fluorescence (3.67 ± 0.10). When we overexpressed an mCherry-tagged dominant-negative form of *Ero*1-Lα (*Ero*1-LαC394S), we observed a lower fluorescence ratio in the ER (2.49 ± 0.04). Furthermore, siRNA mediated downregulation of *Ero*1-Lα with two different siRNAs resulted in the attenuation of the fluorescent signal. These experiments suggested that the H_2O_2 level in the ER is dependent on the activity of *Ero*1-Lα.

The ER of mammalian cells also plays a central role in calcium signaling. We were interested to determine whether the calcium content of the ER has any effect on the oxidative state of this compartment. To study this, we used thapsigargin to deplete the intracellular stores of HeLa cells and studied the HyPer fluorescence in the ER. Figure 4A shows that thapsigargin induced a decrease in fluorescence within 5 min, and

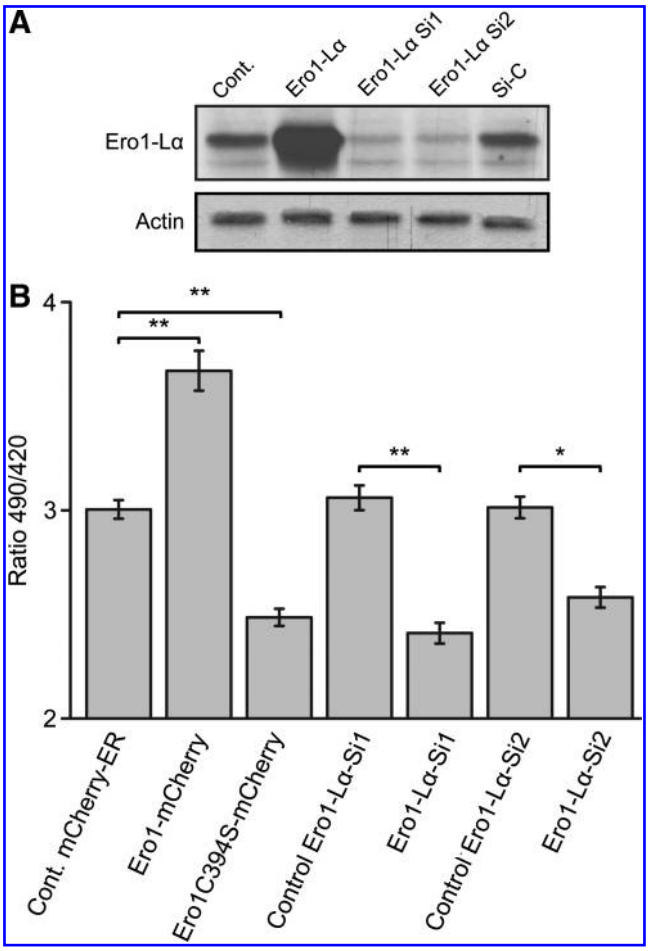

FIG. 3. *Ero*1-Lα regulates the level of H_2O_2 in the ER. (**A**) HeLa cells were transiently transfected with non-tagged *Ero*1-Lα, siRNAs corresponding to *Ero*1-Lα or a medium GC content control siRNA (Si-C), as described in Materials and Methods. Two days after transfection, cell extracts were harvested and subjected to Western-blot analysis of *Ero*1-Lα and beta actin. (**B**) Mean fluorescence ratio of HyPer (490/420 nm) was calculated from 3-min recordings on HeLa cells expressing mCherry-ER ($n = 266$) as a control, *Ero*1-Lα-mCherry ($n = 143$), *Ero*1-Lα C394S-mCherry ($n = 187$), control *Ero*1-Lα-Si1 ($n = 172$), *Ero*1-Lα-Si1 ($n = 190$), control *Ero*1-Lα-Si2 ($n = 153$), and *Ero*1-Lα-Si2 (n = 171). Means ± SEM from three independent experiments on the given number of cells (n) are shown ($^*p < 0.001$, $^{**}p = 0.01$). Average mCherry fluorescence was the same in all experiments.

the signal stabilized at a lower level. Depletion of the intracellular calcium stores induces calcium influx in several cell types mediated by a store-operated pathway (22). Calcium influx, however, was not necessary for inducing the decrease in HyPer fluorescence, because the same change was also observed in the absence of extracellular calcium (data not shown). Figure 4A shows that addition of H_2O_2 to the cells restored the signal to the original level, indicating that a decrease in H_2O_2 concentration was indeed responsible for the thapsigargin-induced decrease of fluorescence. Importantly, the C121S mutant version of HyPer showed little change of fluorescence in response to thapsigargin (Fig. 4A, lower trace).

In our next experiments, we used histamine to induce calcium mobilization in a more physiologic manner. Figure 4B shows that histamine also induced a rapid decrease in intraluminal H_2O_2; however, this signal was transient, and the original fluorescence was restored within 15 min. We managed to follow the changes of cytosolic calcium and intraluminal H_2O_2 in parallel in real time. A representative recording in Fig. 4C shows that thapsigargin elicited an increase in cytosolic calcium originating from store depletion, whereas HyPer fluorescence in the ER permanently decreased. Figure 4D shows that 100 μM histamine induced calcium oscillation with parallel, transient decrease of the HyPer fluorescence. These experiments suggested that calcium mobilization from intracellular stores, either by a receptor agonist or by inhibiting the SERCA, results in relaxation of oxidative state in the ER.

Because previous experiments suggested a role for *Ero*1 in generating H_2O_2 in the ER, we were interested in whether the effect of calcium-store depletion on the ER H_2O_2 level was mediated by a change in *Ero*1 activity. We used an assay based on the detection of intrachain disulfide bonds in J chains under nonreducing conditions to study the activity of *Ero*1 (17). In this assay DTT is used to reduce disulfide bonds in the ER, and the speed of recovery from the reduced state reflects the activity of *Ero*1. To validate the assay, we studied the effects of overexpression and siRNA-mediated depletion of *Ero*1-Lα on the kinetics of recovery. As shown in Fig. 5, overexpression of *Ero*1-Lα accelerated the recovery from the reduced state, whereas the siRNA treatment inhibited J-chain folding after the washout of DTT. Depletion of intracellular stores by thapsigargin, however, had no effect on J-chain folding, suggesting that changes in *Ero*1 activity were not responsible for a calcium-store depletion–induced decrease of H_2O_2 level.

Discussion

Hydrogen peroxide has diverse biologic roles in prokaryotic and eukaryotic organisms. Production of this compound has a well-documented effector role in host defense, fertilization, and hormone biosynthesis, but various signaling functions for H_2O_2 have also emerged recently (25). Several cellular sources of H_2O_2 exist in living organisms. Although intentional H_2O_2 formation is a function of the Nox family of NADPH oxidases (10), H_2O_2 also is formed as a byproduct of mitochondrial respiration (18). Oxidative protein folding in the ER has also been suggested to be a source of H_2O_2; however, surprisingly little information has been gathered about this process over the years.

Reconstitution studies with purified yeast and mammalian *Ero*1 proteins suggested that the enzyme can form H_2O_2; however, it remained unknown whether H_2O_2 is also synthesized in the ER of live cells and whether antioxidant mechanisms can counterbalance the production of H_2O_2. With the help of a recently described protein-based H_2O_2 sensor, HyPer, we demonstrated for the first time that a high level of H_2O_2 exists in the ER of mammalian cells. H_2O_2 sensing by HyPer is based on disulfide-bridge formation between specific cysteine residues of the OxyR core of the protein (6). One can imagine that the increased fluorescence of ER-targeted HyPer may originate from H_2O_2-independent disulfide-bridge formation directly mediated by the *Ero*1/PDI pathway or by a distinct oxidative mechanism. Our results do not exclude this possibility, but several observations suggest that HyPer is indeed a specific sensor for H_2O_2. First, Zheng *et al.* (28) tested the sensing specificity of OxyR by treating *E. coli* cells with several different

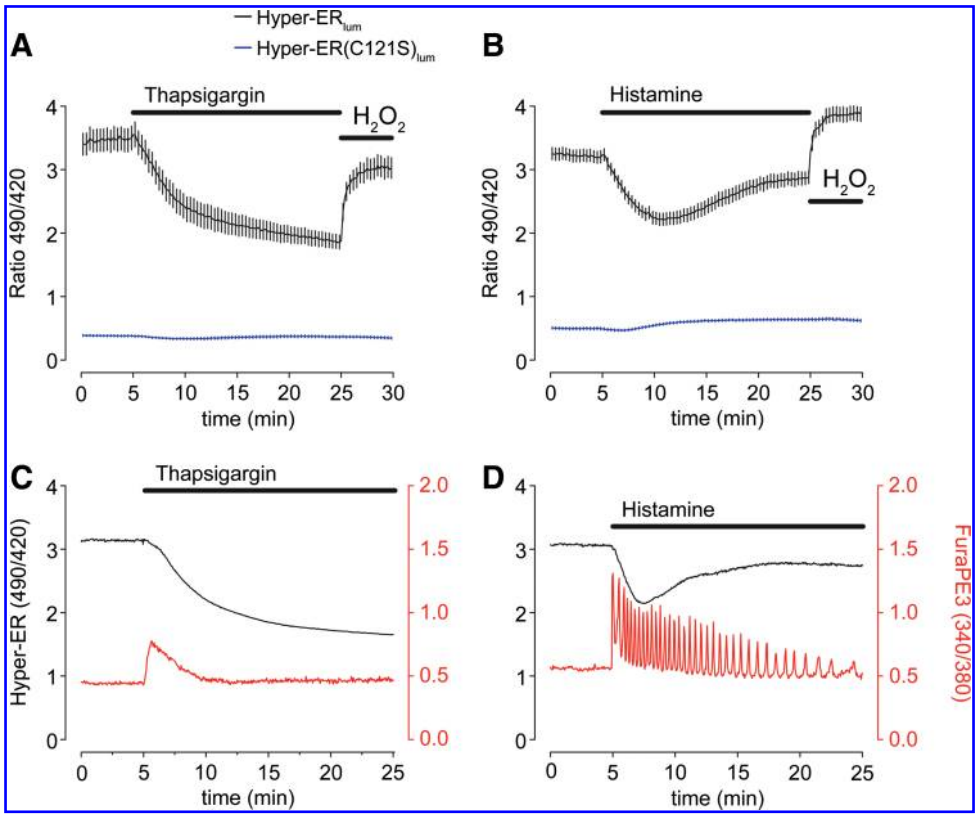

FIG. 4. Calcium mobilization from intracellular stores induces a decrease in ER H_2O_2 level. (**A, B**) Time course of thapsigargin (200 n*M*)- and histamine (100 μM)-induced changes in HyPer-ER$_{lum}$ (black) and HyPer-ER(C121S)$_{lum}$ (blue) fluorescence ratios. Traces are averages ± SEM of 24–34 recordings for thapsigargin and histamine, respectively, from three independent experiments. (**C, D**) Simultaneous imaging of HyPer-ER$_{lum}$ fluorescence (black) and cytosolic Ca^{2+} changes (red) on thapsigargin or histamine stimulation. The left axis represents the excitation ratio of HyPer (490/420), and the right axis, that of Fura-PE3 (340/380). Traces of representative measurements are shown. (For interpretation of the references to color in this figure legend, the reader is referred to the web version of this article at www.liebertonline.com/ars).

oxidants, including H_2O_2, diamide, *S*-nitrosocysteine, nitrite, hydrazine and its derivates, hypochlorous acid and oxidized lipoic acid. Among the tested compounds only H_2O_2 and diamide-activated OxyR, and activation by diamide occurred at concentrations higher than 100 μM. Belousov *et al.* (1) also tested the effect of several oxidants, and only H_2O_2 increased the HyPer fluorescence (1). This remarkable selectivity for H_2O_2 is provided by the structural features of OxyR, the parent molecule for HyPer. Protein crystallographic studies revealed that H_2O_2 sensing by OxyR is mediated by the H_2O_2-mediated oxidation of specific cysteine residues, which are located inside a hydrophobic binding pocket that is accessible only to the small-sized H_2O_2 (6). In agreement with these observations, mutation of a key cysteine residue (Cys^{121}) in ER-targeted HyPer led to a decrease in fluorescence and turned the protein insensitive to changes of H_2O_2. By using specific target sequences, we also mapped H_2O_2 levels at other intracellular locations, and among the sites examined only the mitochondrial matrix showed an increased oxidative state. Interestingly, when HyPer was targeted to the cytoplasmic surface of the ER, its fluorescence was the same as that in the cytosol, indicating that no significant H_2O_2 leak occurs from the ER lumen. Insulating the high H_2O_2 levels is probably of high priority, because H_2O_2 could exert unwanted effects on cytosolic metabolic processes and signaling networks.

To find the origin of the high oxidative state of the ER, we manipulated *Ero*1-Lα expression in Hela cells and found a positive correlation between *Ero*1-Lα expression and H_2O_2 level. These observations establish for the first time a link between *Ero*1-Lα activity and H_2O_2 production in live cells. The observed changes were relatively modest (within 80% of the original signal), which might be explained by the residual protein expression after siRNA treatment and the relative insensitivity of HyPer toward H_2O_2 levels higher than 100 μM (data not shown). Furthermore, when we manipulated *Ero*1-Lα levels, we always measured fluorescence at a new steady state, where the altered *Ero*1-Lα activity might have been counterbalanced by parallel changes in H_2O_2 degradation.

It is also possible that enzymatic sources other than *Ero*1-Lα are responsible for building up high H_2O_2 levels in the ER. For example, an ROS-producing enzyme, NADPH oxidase 4 (Nox4), has been reported to localize to the ER (5, 20). The enzymatic activities of Nox1, Nox2, Nox3, and Nox4 have been reported to be dependent on complex formation with $p22^{phox}$ (11). Complete inhibition of $p22^{phox}$ expression by siRNA treatment did not affect the fluorescence of HyPer-ER$_{lum}$ (data not shown), indicating that Nox enzymes are unlikely to be a source of ROS in the ER of HeLa cells. The contribution of other oxidoreductases, however, cannot be excluded (4). The connection between *Ero*1-Lα activity and

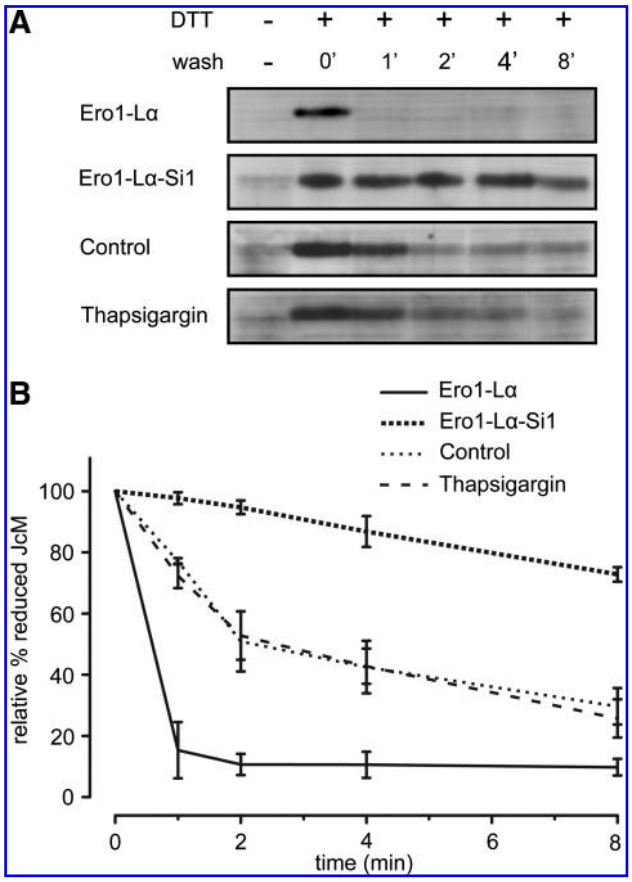

FIG. 5. Oxidative folding of JcM is not regulated by the luminal calcium concentration. (**A**) HeLa cells were transfected for 48 h with V5-tagged J-chain (JcM) alone or in combination with *Ero*1-Lα or *Ero*1-Lα–specific siRNAs. Untreated or thapsigargin (200 n*M*, 20 min)-stimulated cells were then exposed to 10 m*M* DTT for 20 min and monitored for the times indicated without the reducing agent, as described in Materials and Methods. Cell lysates were processed in a standard nonreducing SDS-PAGE and were immunoblotted against V5 epitope. The band representing the reduced form of JcM is shown on the Western blots. (**B**) Intensity of reduced JcM at various time points relative to time 0 min was determined by densitometry. Data represent averages ± SEM from three (Ero1-Lα-Si1) or four experiments (all other conditions).

H_2O_2 production has important potential physiologic and pathophysiologic consequences. Our results suggest that protein folding in cells with high *Ero*1 activity (such as insulin-producing cells of the pancreas) is associated with high intraluminal H_2O_2 production in the ER. Currently, we are studying whether shielding of intraluminal H_2O_2 in secretory cells is effective, similar to that observed in HeLa cells.

Besides its regulation by *Ero*1-Lα, we also found evidence that intraluminal calcium in the ER has a profound effect on the H_2O_2 concentration of the same compartment. Mobilization of calcium from the ER, either by thapsigargin or by the receptor-agonist histamine, resulted in a rapid decrease of H_2O_2 level in the ER.

Currently we have no mechanistic explanation for this effect, but a change in *Ero*1-Lα activity seems unlikely, because thapsigargin did not affect the folding of immunoglobulin J chains, a process that is strictly dependent on the activity of *Ero*1-Lα (17). Furthermore, the amplitude of the thapsigargin-induced decrease of the fluorescence ratio was not affected by the level of *Ero*1-Lα (data not shown). It is possible that instead of regulating the formation of H_2O_2, intraluminal calcium has an effect on the degradation of H_2O_2. Whatever the case may be, the revealed interplay between redox changes and calcium signaling supplements earlier observations, which already suggested a link between the redox state of the ER and calcium handling. Li and Camacho (16) showed that SERCA 2b activity is modulated by CRT and ERp57 oxidoreductases in a redox-state-dependent manner. They also showed that SERCA activity is higher when the ER lumen is in a reduced state, which, according to our observations, develops when calcium content of the ER is depleted. Furthermore, the activity of IP_3 receptor type 1 is also modulated by the redox state of the ER in a way that the reduced state of the ER inhibits Ca^{2+} release through the receptor (14). These data, combined with our observations, fit to a model in which the calcium release induces a more-reduced state of the ER, which then favors restoration of the original calcium content through the parallel inhibition of further calcium release and stimulation of Ca^{2+}-pump activity.

Acknowledgments

We are grateful to Peter Enyedi for his suggestions and to Beata Molnar for technical assistance. This work was supported by grants from the Hungarian Research Fund (OTKA 042573, NF68563, and NF72669) and by grants from the Jedlik Ányos program (1/010/2005) and from the Wellcome Trust.

Author Disclosure Statement

No competing financial interests exist.

References

1. Belousov VV, Fradkov AF, Lukyanov KA, Staroverov DB, Shakhbazov KS, Terskikh AV, and Lukyanov S. Genetically encoded fluorescent indicator for intracellular hydrogen peroxide. *Nat Methods* 3: 281–286, 2006.
2. Cabibbo A, Pagani M, Fabbri M, Rocchi M, Farmery MR, Bulleid NJ, and Sitia R. ERO1-L, a human protein that favors disulfide bond formation in the endoplasmic reticulum. *J Biol Chem* 275: 4827–4833, 2000.
3. Cenci S and Sitia R. Managing and exploiting stress in the antibody factory. *FEBS Lett* 581: 3652–3657, 2007.
4. Chakravarthi S, Jessop CE, Willer M, Stirling CJ, and Bulleid NJ. Intracellular catalysis of disulfide bond formation by the human sulfhydryl oxidase, QSOX1. *Biochem J* 404: 403–411, 2007.
5. Chen K, Kirber MT, Xiao H, Yang Y, and Keaney JF Jr. Regulation of ROS signal transduction by NADPH oxidase 4 localization. *J Cell Biol* 181: 1129–1139, 2008.
6. Choi H, Kim S, Mukhopadhyay P, Cho S, Woo J, Storz G, and Ryu S. Structural basis of the redox switch in the OxyR transcription factor. *Cell* 105: 103–113, 2001.
7. Christman MF, Morgan RW, Jacobson FS, and Ames BN. Positive control of a regulon for defenses against oxidative stress and some heat-shock proteins in *Salmonella typhimurium*. *Cell* 41: 753–762, 1985.
8. Czirjak G and Enyedi P. Targeting of calcineurin to an NFAT-like docking site is required for the calcium-dependent acti-

vation of the background K^+ channel, TRESK. *J Biol Chem* 281: 14677–14682, 2006.
9. Frand AR and Kaiser CA. The ERO1 gene of yeast is required for oxidation of protein dithiols in the endoplasmic reticulum. *Mol Cell* 1: 161–170, 1998.
10. Geiszt M. NADPH oxidases: new kids on the block. *Cardiovasc Res* 71: 289–299, 2006.
11. Geiszt M and Leto TL. The Nox family of NAD(P)H oxidases: host defense and beyond. *J Biol Chem* 279: 51715–51718, 2004.
12. Gross E, Sevier CS, Heldman N, Vitu E, Bentzur M, Kaiser CA, Thorpe C, and Fass D. Generating disulfides enzymatically: reaction products and electron acceptors of the endoplasmic reticulum thiol oxidase Ero1p. *Proc Natl Acad Sci U S A* 103: 299–304, 2006.
13. Hebert DN and Molinari M. In and out of the ER: protein folding, quality control, degradation, and related human diseases. *Physiol Rev* 87: 1377–1408, 2007.
14. Higo T, Hattori M, Nakamura T, Natsume T, Michikawa T, and Mikoshiba K. Subtype-specific and ER luminal environment-dependent regulation of inositol 1,4,5-trisphosphate receptor type 1 by ERp44. *Cell* 120: 85–98, 2005.
15. Inoue T, Heo WD, Grimley JS, Wandless TJ, and Meyer T. An inducible translocation strategy to rapidly activate and inhibit small GTPase signaling pathways. *Nat Methods* 2: 415–418, 2005.
16. Li Y and Camacho P. Ca^{2+}-dependent redox modulation of SERCA 2b by ERp57. *J Cell Biol* 164: 35–46, 2004.
17. Mezghrani A, Fassio A, Benham A, Simmen T, Braakman I, and Sitia R. Manipulation of oxidative protein folding and PDI redox state in mammalian cells. *EMBO J* 20: 6288–6296, 2001.
18. Murphy MP. How mitochondria produce reactive oxygen species. *Biochem J* 417: 1–13, 2009.
19. Pagani M, Fabbri M, Benedetti C, Fassio A, Pilati S, Bulleid NJ, Cabibbo A, and Sitia R. Endoplasmic reticulum oxidoreductin 1-lbeta (ERO1-Lbeta), a human gene induced in the course of the unfolded protein response. *J Biol Chem* 275: 23685–23692, 2000.
20. Petry A, Djordjevic T, Weitnauer M, Kietzmann T, Hess J, and Gorlach A. NOX2 and NOX4 mediate proliferative response in endothelial cells. *Antioxid Redox Signal* 8: 1473–1484, 2006.
21. Pollard MG, Travers KJ, and Weissman JS. Ero1p: a novel and ubiquitous protein with an essential role in oxidative protein folding in the endoplasmic reticulum. *Mol Cell* 1: 171–182, 1998.
22. Putney JW Jr. Recent breakthroughs in the molecular mechanism of capacitative calcium entry (with thoughts on how we got here). *Cell Calcium* 42: 103–110, 2007.
23. Sevier CS and Kaiser CA. Ero1 and redox homeostasis in the endoplasmic reticulum. *Biochim Biophys Acta* 1783: 549–556, 2008.
24. Sirokmany G, Szidonya L, Kaldi K, Gaborik Z, Ligeti E, and Geiszt M. Sec14 homology domain targets p50RhoGAP to endosomes and provides a link between Rab and Rho GTPases. *J Biol Chem* 281: 6096–6105, 2006.
25. Stone JR and Yang S. Hydrogen peroxide: a signaling messenger. *Antioxid Redox Signal* 8: 243–270, 2006.
26. Tu BP and Weissman JS. Oxidative protein folding in eukaryotes: mechanisms and consequences. *J Cell Biol* 164: 341–346, 2004.
27. Wang L, Li SJ, Sidhu A, Zhu L, Liang Y, Freedman RB, and Wang CC. Reconstitution of human Ero1-Lalpha/protein-disulfide isomerase oxidative folding pathway in vitro: position-dependent differences in role between the a and a' domains of protein-disulfide isomerase. *J Biol Chem* 284: 199–206, 2009.
28. Zheng M, Aslund F, and Storz G. Activation of the OxyR transcription factor by reversible disulfide bond formation. *Science* 279: 1718–1721, 1998.

Address correspondence to:
Miklós Geiszt
Department of Physiology
Semmelweis University
Faculty of Medicine
PO Box 259
H-1444 Budapest
Hungary

E-mail: geiszt@puskin.sote.hu

Date of first submission to ARS Central, September 8, 2009; date of final revised submission, January 6, 2010; date of acceptance, January 22, 2010.

Abbreviations Used

DMEM = Dulbecco's modified Eagle's medium
DTT = dithiothreitol
ER = endoplasmic reticulum
*Ero*1 = endoplasmic reticulum oxidoreductin 1
FAD = flavin adenine dinucleotide
GFP = green fluorescent protein
HEPES = 4-(2-hydroxyethyl)-1-piperazineethanesulfonic acid
IP_3 = inositol-1,4,5-trisphosphate
JcM = modified murine J chain
NADPH = nicotinamide adenine dinucleotide phosphate
NEM = *N*-ethyl maleimide
Nox = NADPH oxidase
PBS = phosphate-buffered saline
PDI = protein disulfide isomerase
RFP = red fluorescent protein
RNAi = RNA interference
ROS = reactive oxygen species
SDS-PAGE = sodium dodecylsulfate polyacrylamide gel electrophoresis
SEM = standard error of the mean
SERCA = sarco-endoplasmic reticulum calcium ATPase
siRNA = small inhibitory RNA
SV40 = simian vacuolating virus 40
Tris = *tris*(hydroxymethyl)aminomethane
VH chain = variable region heavy chain

This article has been cited by:

1. Ilir Mehmeti, Stephan Lortz, Sigurd Lenzen. 2012. The H2O2-sensitive HyPer protein targeted to the endoplasmic reticulum as a mirror of the oxidizing thiol–disulfide milieu. *Free Radical Biology and Medicine* **53**:7, 1451-1458. [CrossRef]
2. Zoltán Spiró , Mehmet Alper Arslan , Milán Somogyvári , Minh Tu Nguyen , Arne Smolders , Balázs Dancsó , Nóra Németh , Zsuzsanna Elek , Bart P. Braeckman , Péter Csermely , Csaba S#ti . 2012. RNA Interference Links Oxidative Stress to the Inhibition of Heat Stress Adaptation. *Antioxidants & Redox Signaling* **17**:6, 890-901. [Abstract] [Full Text HTML] [Full Text PDF] [Full Text PDF with Links] [Supplemental material]
3. Catherine I. Andreu, Ute Woehlbier, Mauricio Torres, Claudio Hetz. 2012. Protein disulfide isomerases in neurodegeneration: From disease mechanisms to biomedical applications. *FEBS Letters* **586**:18, 2826-2834. [CrossRef]
4. Milena Bertolotti , Roberto Sitia , Anna Rubartelli . 2012. On the Redox Control of B Lymphocyte Differentiation and Function. *Antioxidants & Redox Signaling* **16**:10, 1139-1149. [Abstract] [Full Text HTML] [Full Text PDF] [Full Text PDF with Links]
5. Éva Margittai , Péter Löw , Ibolya Stiller , Alessandra Greco , Jose Manuel Garcia-Manteiga , Niccolo Pengo , Angelo Benedetti , Roberto Sitia , Gábor Bánhegyi . 2012. Production of H2O2 in the Endoplasmic Reticulum Promotes In Vivo Disulfide Bond Formation. *Antioxidants & Redox Signaling* **16**:10, 1088-1099. [Abstract] [Full Text HTML] [Full Text PDF] [Full Text PDF with Links] [Supplemental material]
6. Lloyd W. Ruddock . 2012. Low-Molecular-Weight Oxidants Involved in Disulfide Bond Formation. *Antioxidants & Redox Signaling* **16**:10, 1129-1138. [Abstract] [Full Text HTML] [Full Text PDF] [Full Text PDF with Links]
7. Christian Appenzeller-Herzog . 2012. Updates on “Endoplasmic Reticulum Redox”. *Antioxidants & Redox Signaling* **16**:8, 760-762. [Citation] [Full Text HTML] [Full Text PDF] [Full Text PDF with Links]
8. Taichi Kakihana , Kazuhiro Nagata , Roberto Sitia . 2012. Peroxides and Peroxidases in the Endoplasmic Reticulum: Integrating Redox Homeostasis and Oxidative Folding. *Antioxidants & Redox Signaling* **16**:8, 763-771. [Abstract] [Full Text HTML] [Full Text PDF] [Full Text PDF with Links]
9. Raz Palty, Adi Raveh, Ido Kaminsky, Ruth Meller, Eitan Reuveny. 2012. SARAF Inactivates the Store Operated Calcium Entry Machinery to Prevent Excess Calcium Refilling. *Cell* **149**:2, 425-438. [CrossRef]
10. GRAHAM NOCTOR, AMNA MHAMDI, SEJIR CHAOUCH, YI HAN, JENNY NEUKERMANS, BELEN MARQUEZ-GARCIA, GUILLAUME QUEVAL, CHRISTINE H. FOYER. 2012. Glutathione in plants: an integrated overview. *Plant, Cell & Environment* **35**:2, 454-484. [CrossRef]
11. Franziska Kriegenburg , Esben G. Poulsen , Annett Koch , Elke Krüger , Rasmus Hartmann-Petersen . 2011. Redox Control of the Ubiquitin-Proteasome System: From Molecular Mechanisms to Functional Significance. *Antioxidants & Redox Signaling* **15**:8, 2265-2299. [Abstract] [Full Text HTML] [Full Text PDF] [Full Text PDF with Links]
12. M R Amoroso, D S Matassa, G Laudiero, A V Egorova, R S Polishchuk, F Maddalena, A Piscazzi, S Paladino, D Sarnataro, C Garbi, M Landriscina, F Esposito. 2011. TRAP1 and the proteasome regulatory particle TBP7/Rpt3 interact in the endoplasmic reticulum and control cellular ubiquitination of specific mitochondrial proteins. *Cell Death and Differentiation* . [CrossRef]
13. Junichi Fujii, Satoshi Tsunoda. 2011. Redox regulation of fertilisation and the spermatogenic process. *Asian Journal of Andrology* **13**:3, 420-423. [CrossRef]
14. Michael P. Murphy, Arne Holmgren, Nils-Göran Larsson, Barry Halliwell, Christopher J. Chang, Balaraman Kalyanaraman, Sue Goo Rhee, Paul J. Thornalley, Linda Partridge, David Gems, Thomas Nyström, Vsevolod Belousov, Paul T. Schumacker, Christine C. Winterbourn. 2011. Unraveling the Biological Roles of Reactive Oxygen Species. *Cell Metabolism* **13**:4, 361-366. [CrossRef]
15. Y. Ikeda, M. Nakano, H. Ihara, R. Ito, N. Taniguchi, J. Fujii. 2011. Different consequences of reactions with hydrogen peroxide and t-butyl hydroperoxide in the hyperoxidative inactivation of rat peroxiredoxin-4. *Journal of Biochemistry* **149**:4, 443-453. [CrossRef]
16. Van Dat Nguyen, Mirva J. Saaranen, Anna-Riikka Karala, Anna-Kaisa Lappi, Lei Wang, Irina B. Raykhel, Heli I. Alanen, Kirsi E.H. Salo, Chih-chen Wang, Lloyd W. Ruddock. 2011. Two Endoplasmic Reticulum PDI Peroxidases Increase the Efficiency of the Use of Peroxide during Disulfide Bond Formation. *Journal of Molecular Biology* **406**:3, 503-515. [CrossRef]
17. Natalia M. Mishina , Pyotr A. Tyurin-Kuzmin , Kseniya N. Markvicheva , Alexander V. Vorotnikov , Vsevolod A. Tkachuk , Vibor Laketa , Carsten Schultz , Sergey Lukyanov , Vsevolod V. Belousov . 2011. Does Cellular Hydrogen Peroxide Diffuse or Act Locally?. *Antioxidants & Redox Signaling* **14**:1, 1-7. [Abstract] [Full Text HTML] [Full Text PDF] [Full Text PDF with Links] [Supplemental material]

18. Éva Margittai, Roberto Sitia. 2011. Oxidative Protein Folding in the Secretory Pathway and Redox Signaling Across Compartments and Cells. *Traffic* **12**:1, 1-8. [CrossRef]
19. Ester Zito, Eduardo Pinho Melo, Yun Yang, Åsa Wahlander, Thomas A. Neubert, David Ron. 2010. Oxidative Protein Folding by an Endoplasmic Reticulum-Localized Peroxiredoxin. *Molecular Cell* **40**:5, 787-797. [CrossRef]
20. Roberta Vené , Laura Delfino , Patrizia Castellani , Enrica Balza , Milena Bertolotti , Roberto Sitia , Anna Rubartelli . 2010. Redox Remodeling Allows and Controls B-Cell Activation and Differentiation. *Antioxidants & Redox Signaling* **13**:8, 1145-1155. [Abstract] [Full Text HTML] [Full Text PDF] [Full Text PDF with Links] [Supplemental material]
21. Christian Appenzeller-Herzog, Jan Riemer, Ester Zito, King-Tung Chin, David Ron, Martin Spiess, Lars Ellgaard. 2010. Disulphide production by Ero1#–PDI relay is rapid and effectively regulated. *The EMBO Journal* **29**:19, 3318-3329. [CrossRef]
22. Thomas Simmen, Emily M. Lynes, Kevin Gesson, Gary Thomas. 2010. Oxidative protein folding in the endoplasmic reticulum: Tight links to the mitochondria-associated membrane (MAM). *Biochimica et Biophysica Acta (BBA) - Biomembranes* **1798**:8, 1465-1473. [CrossRef]